Help us improve our products. Sign up to take part.

- Letter
- Published: 01 May 2008

The missing memristor found

Dmitri B. Strukov, Gregory S. Snider, Duncan R. Stewart & R. Stanley Williams

Nature **453**, 80–83 (2008)

- A Corrigendum to this article was published on 25 June 2009

Abstract

Anyone who ever took an electronics laboratory class will be familiar with the fundamental passive circuit elements: the resistor, the capacitor and the inductor. However, in 1971 Leon Chua reasoned from symmetry arguments that there should be a fourth fundamental element, which he called a memristor (short for memory resistor)[1]. Although he showed that such an element has many interesting and valuable circuit properties, until now no one has presented either a useful physical model or an example of a memristor. Here we show, using a simple analytical example, that memristance arises naturally in nanoscale systems in which solid-state electronic and ionic transport are coupled under an external bias voltage. These results serve as the foundation for understanding a wide range of hysteretic current–voltage behaviour observed in many nanoscale electronic devices[2,3,4,5,6,7,8,9,10,11,12,13,14,15,16,17,18,19] that involve the motion of charged atomic or molecular species, in particular certain titanium dioxide cross-point switches[20,21,22].

Access provided by Chonbuk National University

Main

More specifically, Chua noted that there are six different mathematical relations connecting pairs of the four fundamental circuit variables: electric current i, voltage v, charge q and magnetic flux ϕ. One of these relations (the charge is the time integral of the current) is determined from the definitions of two of the variables, and another (the flux is the time integral of the electromotive force, or voltage) is determined from Faraday's law of induction. Thus, there should be four basic circuit elements described by the remaining relations between the variables (Fig. 1). The 'missing' element—the memristor, with memristance M—provides a functional relation between charge and flux, $d\phi = M dq$.

Figure 1: The four fundamental two-terminal circuit elements: resistor, capacitor, inductor and memristor.

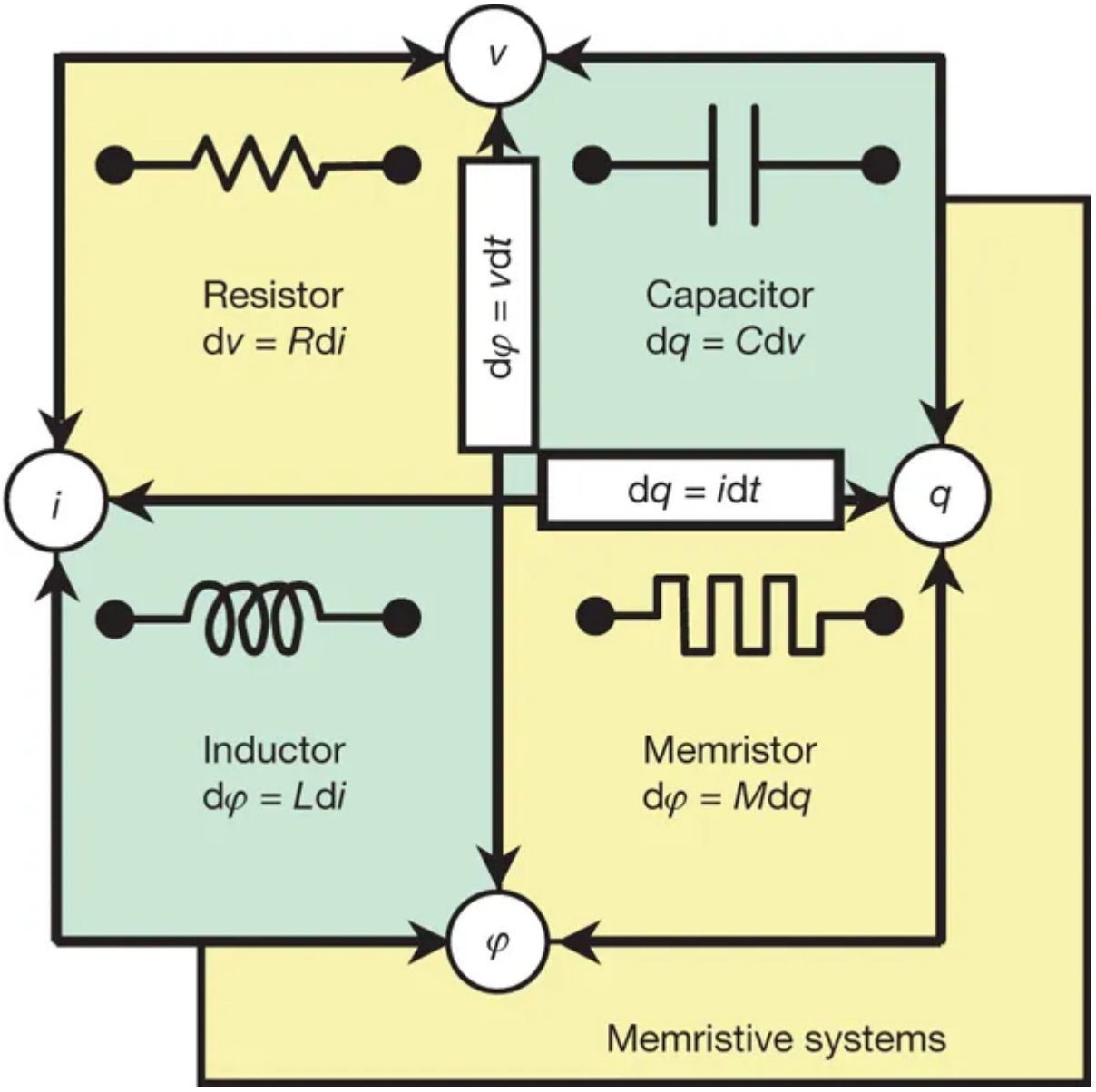

Resistors and memristors are subsets of a more general class of dynamical devices, memristive systems. Note that R, C, L and M can be functions of the independent variable in their defining equations, yielding nonlinear elements. For example, a charge-controlled memristor is defined by a single-valued function $M(q)$.

In the case of linear elements, in which M is a constant, memristance is identical to resistance and, thus, is of no special interest. However, if M is itself a function of q, yielding a nonlinear circuit element, then the situation is more interesting. The i–v characteristic of

such a nonlinear relation between q and ϕ for a sinusoidal input is generally a frequency-dependent Lissajous figure[1], and no combination of nonlinear resistive, capacitive and inductive components can duplicate the circuit properties of a nonlinear memristor (although including active circuit elements such as amplifiers can do so)[1]. Because most valuable circuit functions are attributable to nonlinear device characteristics, memristors compatible with integrated circuits could provide new circuit functions such as electronic resistance switching at extremely high two-terminal device densities. However, until now there has not been a material realization of a memristor.

The most basic mathematical definition of a current-controlled memristor for circuit analysis is the differential form

$$v = \mathcal{R}(w)i \quad (1)$$

$$\frac{dw}{dt} = i \quad (2)$$

where w is the state variable of the device and $\mathcal{R}$ is a generalized resistance that depends upon the internal state of the device. In this case the state variable is just the charge, but no one has been able to propose a physical model that satisfies these simple equations. In 1976 Chua and Kang generalized the memristor concept to a much broader class of nonlinear dynamical systems they called memristive systems[23], described by the equations

$$v = \mathcal{R}(w,i)i \quad (3)$$

$$\frac{dw}{dt} = f(w,i) \quad (4)$$

where w can be a set of state variables and $\mathcal{R}$ and f can in general be explicit functions of time. Here, for simplicity, we restrict the discussion to current-controlled, time-invariant, one-port devices. Note that, unlike in a memristor, the flux in memristive systems is no longer uniquely defined by the charge. However, equation (3) does serve to distinguish a memristive system from an arbitrary dynamical device; no current flows through the memristive system when the voltage drop across it is zero. Chua and Kang showed that the i–v characteristics of some devices and systems, notably thermistors, Josephson junctions, neon bulbs and even the Hodgkin–Huxley model of the neuron, can be modelled using memristive equations[23]. Nevertheless, there was no direct connection between the mathematics and the physical properties of any practical system, and hence, almost forty years later, the concepts have not been widely adopted.

Here we present a physical model of a two-terminal electrical device that behaves like a perfect memristor for a certain restricted range of the state variable w and as a memristive system for another, wider (but still bounded), range of w. This intuitive model produces rich hysteretic behaviour controlled by the intrinsic nonlinearity of M and the boundary conditions on the state variable w. The results provide a simplified explanation for reports of current–voltage anomalies, including switching and hysteretic conductance, multiple conductance states and apparent negative differential resistance, especially in thin-film, two-terminal nanoscale devices, that have been appearing in the literature for nearly 50 years[2,3,4].

Electrical switching in thin-film devices has recently attracted renewed attention, because such a technology may enable functional scaling of logic and memory circuits well beyond the limits of complementary metal–oxide–semiconductors[24,25]. The microscopic nature of resistance switching and charge transport in such devices is still under debate, but one proposal is that the hysteresis requires some sort of atomic rearrangement that modulates the electronic current. On the basis of this proposition, we consider a thin semiconductor film of thickness D sandwiched between two metal contacts, as shown in Fig. 2a. The total resistance of the device is determined by two variable resistors connected in series (Fig. 2a), where the resistances are given for the full length D of the device. Specifically, the semiconductor film has a region with a high concentration of dopants (in this example assumed to be positive ions) having low resistance $\mathcal{R}_{\mathrm{ON}}$, and the remainder has a low (essentially zero) dopant concentration and much higher resistance $\mathcal{R}_{\mathrm{OFF}}$.

Figure 2: The coupled variable-resistor model for a memristor.

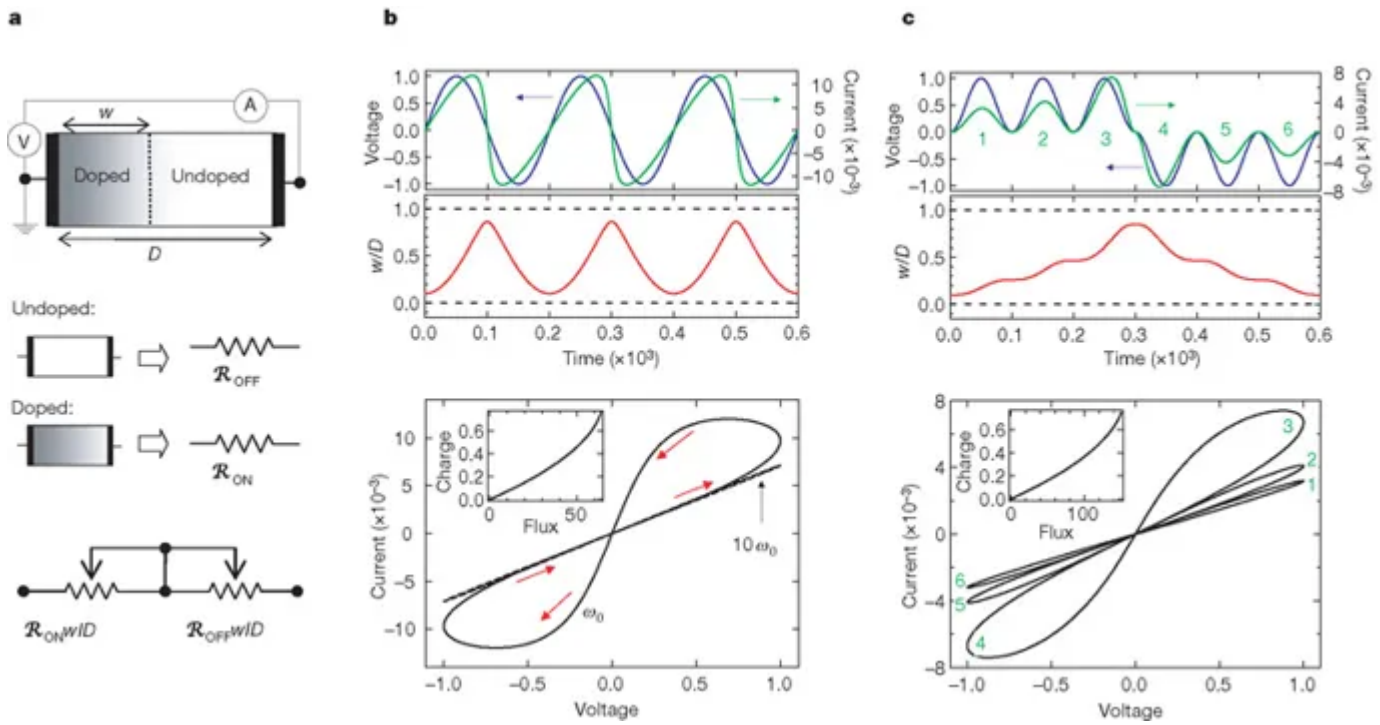

a, Diagram with a simplified equivalent circuit. V, voltmeter; A, ammeter. b, c, The applied voltage (blue) and resulting current (green) as a function of time t for a typical memristor. In b the applied voltage is $v_0\sin(\omega_0 t)$ and the resistance ratio is $\mathcal{R}_{OFF}/\mathcal{R}_{ON} = 160$, and in c the applied voltage is $\pm v_0\sin^2(\omega_0 t)$ and $\mathcal{R}_{OFF}/\mathcal{R}_{ON} = 380$, where v_0 is the magnitude of the applied voltage and ω_0 is the frequency. The numbers 1–6 label successive waves in the applied voltage and the corresponding loops in the i–v curves. In each plot the axes are dimensionless, with voltage, current, time, flux and charge expressed in units of $v_0 = 1$ V, $i_0 \equiv v_0/\mathcal{R}_{ON} = 10$ mA, $t_0 \equiv 2\pi/\omega_0 \equiv D^2/\mu_V v_0 = 10$ ms, $v_0 t_0$ and $i_0 t_0$, respectively. Here i_0 denotes the maximum possible current through the device, and t_0 is the shortest time required for linear drift of dopants across the full device length in a uniform field v_0/D, for example with $D = 10$ nm and $\mu_V = 10^{-10}$ cm^2 s^{-1} V^{-1}. We note that, for the parameters chosen, the applied bias never forces either of the two resistive regions to collapse; for example, w/D does not approach zero or one (shown with dashed lines in the middle plots in b and c). Also, the dashed i–v plot in b demonstrates the hysteresis collapse observed with a tenfold increase in sweep frequency. The insets in the i–v plots in b and c show that for these examples the charge is a single-valued function of the flux, as it must be in a memristor.

The application of an external bias $v(t)$ across the device will move the boundary between the two regions by causing the charged dopants to drift[26]. For the simplest case of ohmic electronic conduction and linear ionic drift in a uniform field with average ion mobility μ_V, we obtain

$$v(t) = \left(\mathcal{R}_{ON}\frac{w(t)}{D} + \mathcal{R}_{OFF}\left(1 - \frac{w(t)}{D}\right)\right) i(t) \quad (5)$$

$$\frac{dw(t)}{dt} = \mu_V \frac{\mathcal{R}_{ON}}{D} i(t) \quad (6)$$

which yields the following formula for $w(t)$:

$$w(t) = \mu_V \frac{\mathcal{R}_{ON}}{D} q(t) \quad (7)$$

By inserting equation (7) into equation (5) we obtain the memristance of this system, which for $\mathcal{R}_{ON} \ll \mathcal{R}_{OFF}$ simplifies to:

$$M(q) = \mathcal{R}_{OFF}\left(1 - \frac{\mu_V \mathcal{R}_{ON}}{D^2} q(t)\right)$$

The q-dependent term in parentheses on the right-hand side of this equation is the crucial contribution to the memristance, and it becomes larger in absolute value for higher dopant mobilities μ_V and smaller semiconductor film thicknesses D. For any material, this term is 1,000,000 times larger in absolute value at the nanometre scale than it is at the micrometre scale, because of the factor of $1/D^2$, and the memristance is correspondingly more significant. Thus, memristance becomes more important for understanding the electronic characteristics of any device as the critical dimensions shrink to the nanometre scale.

The coupled equations of motion for the charged dopants and the electrons in this system take the normal form for a current-controlled (or charge-controlled) memristor (equations (1) and (2)). The fact that the magnetic field does not play an explicit role in the mechanism of memristance is one possible reason why the phenomenon has been hidden for so long; those interested in memristive devices were searching in the wrong places. The mathematics simply require there to be a nonlinear relationship between the integrals of the current and voltage, which is realized in equations (5) and (6). Another significant issue that was not anticipated by Chua is that the state variable w, which in this case specifies the distribution of dopants in the device, is bounded between zero and D. The state variable is proportional to the charge q that passes through the device until its value approaches D;

this is the condition of 'hard' switching (large voltage excursions or long times under bias). As long as the system remains in the memristor regime, any symmetrical alternating-current voltage bias results in double-loop i–v hysteresis that collapses to a straight line for high frequencies (Fig. 2b). Multiple continuous states will also be obtained if there is any sort of asymmetry in the applied bias (Fig. 2c).

Obviously, equation (7) is only valid for values of w in the interval $[0, D]$. Different hard-switching cases are defined by imposing a variety of boundary conditions, such as assuming that once the value of w reaches either of the boundaries, it remains constant until the voltage reverses polarity. In such a case, the device satisfies the normal equations for a current-controlled memristive system (equations (3) and (4)). Figure 3a, b shows two qualitatively different i–v curves that are possible for such a memristive device. In Fig. 3a, the upper boundary is reached while the derivative of the voltage is negative, producing an apparent or 'dynamical' negative differential resistance. Unlike a true 'static' negative differential resistance, which would be insensitive to time and device history, such a dynamical effect is simply a result of the charge-dependent change in the device resistance, and can be identified by a strong dependence on the frequency of a sinusoidal driving voltage. In another case, for example when the boundary is reached much faster by doubling the magnitude of the applied voltage (Fig. 3b), the switching event is a monotonic function of current. Even though in the hard-switching case there appears to be a clearly defined threshold voltage for switching from the 'off' (high resistance) state to the 'on' (low resistance) state, the effect is actually dynamical. This means that any positive voltage v_+ applied to the device in the off state will eventually switch it to the on state after time $\sim D^2\mathcal{R}_{\mathrm{OFF}}/(2\mu_{\mathrm{V}}v_+\mathcal{R}_{\mathrm{ON}})$. The device will remain in the on state as long as a positive voltage is applied, but even a small negative bias will switch it back to the off state; this is why a current-hysteresis loop is only observed for the positive voltage sweep in Fig. 3a, b.

Figure 3: Simulations of a voltage-driven memristive device.

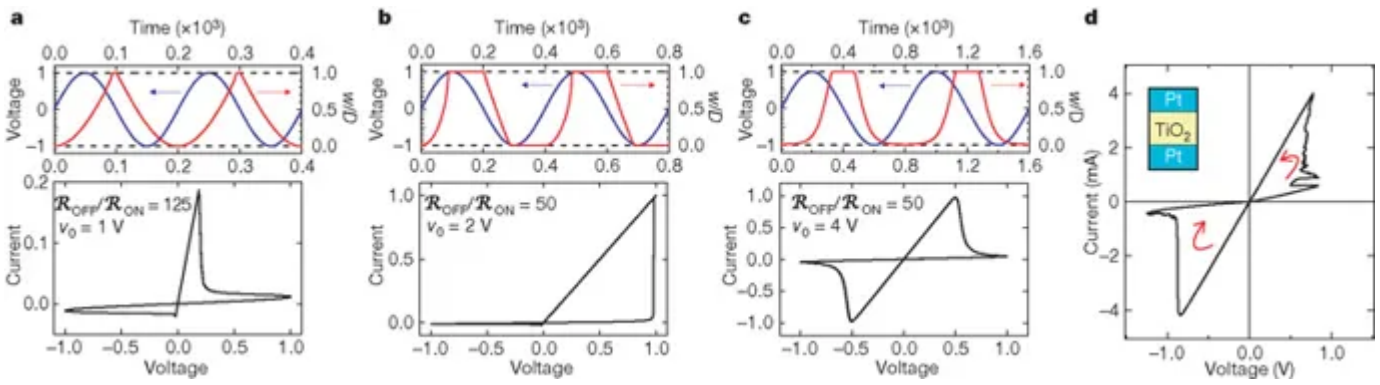

a, Simulation with dynamic negative differential resistance; b, simulation with no dynamic negative differential resistance; c, simulation governed by nonlinear ionic drift. In the upper plots of a, b and c we plot the voltage stimulus (blue) and the corresponding change in the normalized state variable w/D (red), versus time. In all cases, hard switching occurs when w/D closely approaches the boundaries at zero and one (dashed), and the qualitatively different i–v hysteresis shapes are due to the specific dependence of w/D on the electric field near the boundaries. d, For comparison, we present an experimental i–v plot of a Pt–TiO_{2-x}–Pt device[21].

In nanoscale devices, small voltages can yield enormous electric fields, which in turn can produce significant nonlinearities in ionic transport. Figure 3c illustrates such a case in which the right-hand side of equation (6) is multiplied by a window function $w(1 - w)/D^2$, which corresponds to nonlinear drift when w is close to zero or D. In this case, the switching event requires a significantly larger amount of charge (or even a threshold voltage) in order for w to approach either boundary. Therefore, the switching is essentially binary because the on and off states can be held much longer if the voltage does not exceed a specific threshold. Nonlinearity can also be expected in the electronic transport, which can be due to, for example, tunnelling at the interfaces or high-field electron hopping. In this case, the hysteresis behaviour discussed above remains essentially the same but the i–v characteristic becomes nonlinear.

The model of equations (5) and (6) exhibits many features that have been described as bipolar switching, that is, when voltages of opposite polarity are required for switching a device to the on state and the off state. This type of behaviour has been experimentally

observed in various material systems: organic films[5,6,7,8,9] that contain charged dopants or molecules with mobile charged components; chalcogenides[4,10,11,12], where switching is attributed to ion migration rather than a phase transition; and metal oxides[2,3,4,20], notably TiO_2 (refs 4, 13, 14, 21) and various perovskites[4,15,16,17,18,19]. For example, multi-state[8,9,10,11,12,13,14,16,17,18,20,21] and binary[3,4,7,15,16] switching that are similar to those modelled in Figs 2c and 3c, respectively, have been observed, with some showing dynamical negative differential resistance. Typically, hysteresis such as in Fig. 3c is observed for both voltage polarities[7,9,10,11,12,14,15,16,17,21], but observations of i–v characteristics resembling Fig. 3a, b have also been reported[8,17,18,19,20]. In our own studies of TiO_x devices, i–v behaviours very similar to those in Figs 2b, 2c and 3c are regularly observed. Figure 3d illustrates an experimental i–v characteristic from a metal/oxide/metal cross-point device within which the critical 5-nm-thick oxide film initially contained one layer of insulating TiO_2 and one layer of oxygen-poor TiO_{2-x} (refs 21, 22). In this system, oxygen vacancies act as mobile +2-charged dopants, which drift in the applied electric field, shifting the dividing line between the TiO_2 and TiO_{2-x} layers. The switching characteristic observed for a particular memristive system helps classify the nature of the boundary conditions on the state variable of the device.

The rich hysteretic i–v characteristics detected in many thin-film, two-terminal devices can now be understood as memristive behaviour defined by coupled equations of motion: some for (ionized) atomic degrees of freedom that define the internal state of the device, and others for the electronic transport. This behaviour is increasingly relevant as the active region in many electronic devices continues to shrink to a width of only a few nanometres, so even a low applied voltage corresponds to a large electric field that can cause charged species to move. Such dopant or impurity motion through the active region can produce dramatic changes in the device resistance. Including memristors and memristive systems in integrated circuits has the potential to significantly extend circuit functionality as long as the dynamical nature of such devices is understood and properly used. Important applications include ultradense, semi-non-volatile memories and learning networks that require a synapse-like function.

References

1 Chua, L. O. Memristor - the missing circuit element. *IEEE Trans. Circuit Theory* **18**, 507–519 (1971)

2 Hickmott, M. T. Low-frequency negative resistance in thin anodic oxide films. *J. Appl. Phys.* **33**, 2669–2682 (1962)

3 Dearnaley, G., Stoneham, A. M. & Morgan, D. V. Electrical phenomena in amorphous oxide films. *Rep. Prog. Phys.* **33**, 1129–1192 (1970)

4 Waser, R. & Aono, M. Nanoionics-based resistive switching memories. *Nature Mater.* **6**, 833–840 (2007)

5 Scott, J. C. & Bozano, L. D. Nonvolatile memory elements based on organic materials. *Adv. Mater.* **19**, 1452–1463 (2007)

6 Collier, C. P. et al. A [2]catenane-based solid state electronically reconfigurable switch. *Science* **289**, 1172–1175 (2000)

7 Zhitenev, N. B., Sidorenko, A., Tennant, D. M. & Cirelli, R. A. Chemical modification of the electronic conducting states in polymer nanodevices. *Nature Nanotechnol.* **2**, 237–242 (2007)

8 Smits, J. H. A., Meskers, S. C. J., Janssen, R. A. J., Marsman, A. W. & de Leeuw, D. M. Electrically rewritable memory cells from poly(3-hexylthiophene) Schottky diodes. *Adv. Mater.* **17**, 1169–1173 (2005)

9 Lai, Q. X., Zhu, Z. H., Chen, Y., Patil, S. & Wudl, F. Organic nonvolatile memory by dopant-configurable polymer. *Appl. Phys. Lett.* **88**, 133515 (2006)

10 Terabe, K., Hasegawa, T., Nakayama, T. & Aono, M. Quantized conductance atomic switch. *Nature* **433**, 47–50 (2005)

11 Kozicki, M. N., Park, M. & Mitkova, M. Nanoscale memory elements based on solid-state electrolytes. *IEEE Trans. Nanotechnol.* **4**, 331–338 (2005)

12 Dietrich, S. et al. A nonvolatile 2-Mbit CBRAM memory core featuring advanced read and program control. *IEEE J. Solid State Circuits* **42**, 839–845 (2007)

13 Jameson, J. R. et al. Field-programmable rectification in rutile TiO2 crystals. *Appl. Phys. Lett.* **91**, 112101 (2007)

14 Jeong, D. S., Schroeder, H. & Waser, R. Coexistence of bipolar and unipolar resistive switching behaviors in a Pt/TiO2/Pt stack. *Electrochem. Solid State Lett.* **10**, G51–G53 (2007)

15 Beck, A., Bednorz, J. G., Gerber, C., Rossel, C. & Widmer, D. Reproducible switching effect in thin oxide films for memory applications. *Appl. Phys. Lett.* **77**, 139–141 (2000)

16 Szot, K., Speier, W., Bihlmayer, G. & Waser, R. Switching the electrical resistance of individual dislocations in single-crystalline SrTiO3 . *Nature Mater.* **5**, 312–320 (2006)

17 Sawa, A., Fujii, T., Kawasaki, M. & Tokura, Y. Interface resistance switching at a few nanometer thick perovskite manganite active layers. *Appl. Phys. Lett.* **88**, 232112 (2006)

18 Hamaguchi, M., Aoyama, K., Asanuma, S., Uesu, Y. & Katsufuji, T. Electric-field-induced resistance switching universally observed in transition-metal-oxide thin films. *Appl. Phys. Lett.* **88**, 142508 (2006)

19 Oligschlaeger, R., Waser, R., Meyer, R., Karthauser, S. & Dittmann, R. Resistive switching and data reliability of epitaxial (Ba,Sr)TiO3 thin films. *Appl. Phys. Lett.* **88**, 042901 (2006)

20 Richter, C. A., Stewart, D. R., Ohlberg, D. A. A. & Williams, R. S. Electrical characterization of Al/AlO *x* /molecule/Ti/Al devices. *Appl. Phys. Mater. Sci. Process.* **80**, 1355–1362 (2005)

21 Stewart, D. R. et al. Molecule-independent electrical switching in Pt/organic monolayer/Ti devices. *Nano Lett.* **4**, 133–136 (2004)

22 Blackstock, J. J., Stickle, W. F., Donley, C. L., Stewart, D. R. & Williams, R. S. Internal structure of a molecular junction device: chemical reduction of PtO2 by Ti evaporation onto

an interceding organic monolayer. *J. Phys. Chem. C* **111**, 16–20 (2007)

23 Chua, L. O. & Kang, S. M. Memristive devices and systems. *Proc. IEEE* **64**, 209–223 (1976)

24 Kuekes, P. J., Snider, G. S. & Williams, R. S. Crossbar nanocomputers. *Sci. Am.* **293**, 72–78 (2005)

25 Strukov, D. B. & Likharev, K. K. Defect-tolerant architectures for nanoelectronic crossbar memories. *J. Nanosci. Nanotechnol.* **7**, 151–167 (2007)

26 Blanc, J. & Staebler, D. L. Electrocoloration in SrTiO - vacancy drift and oxidation-reduction of transition metals. *Phys. Rev. B* **4**, 3548–3557 (1971)

Acknowledgements

This research was conducted with partial support from DARPA and DTO.

Author information

Affiliations

HP Labs, 1501 Page Mill Road, Palo Alto, California 94304, USA
Dmitri B. Strukov, Gregory S. Snider, Duncan R. Stewart & R. Stanley Williams

Corresponding author

Correspondence to R. Stanley Williams.

Rights and permissions

Reprints and Permissions

About this article

Received **Accepted** **Issue Date** **DOI**
06 December 200717 March 200801 May 2008https://doi.org/10.1038/nature06932

Share this article

Anyone you share the following link with will be able to read this content:

Get shareable link

Further reading

Parasitic Memcapacitor Effects on HP TiO2 Memristor Dynamics - ***https://doi.org/10.1109/ACCESS.2019.2914938***
Yiran Shen, Guangyi Wang, Yan Liang, Simin Yu[…]Herbert Ho-Ching Iu

IEEE Access (2019)

General fractional order mem-elements mutators - ***https://doi.org/10.1016/j.mejo.2019.05.018***
Nariman A. Khalil, Lobna A. Said, Ahmed G. Radwan[…]Ahmed M. Soliman

Microelectronics Journal (2019)

Ge/Oxide Structured Programmable Phototransistors - ***https://doi.org/10.1109/LED.2019.2897817***
Bing Chen, Shun Xu, Ran Cheng[…]Yi Zhao

IEEE Electron Device Letters (2019)

Resistive switching and synaptic properties modifications in gallium-doped zinc oxide memristive devices - ***https://doi.org/10.1016/j.rinp.2019.02.034***

Shilpa S. More, Pratiksha A. Patil, Kalyani D. Kadam, Harshada S. Patil, Snehal L. Patil, Aishwarya V. Pawar, Sharon S. Kanapally, Dhanashri V. Desai, Shraddha M. Bodake, Rajanish K. Kamat, Sungjun Kim[…]Tukaram D. Dongale

Results in Physics (2019)

Nitrogen-Induced Enhancement of Synaptic Weight Reliability in Titanium Oxide-Based Resistive Artificial Synapse and Demonstration of the Reliability Effect on the Neuromorphic System - ***https://doi.org/10.1021/acsami.9b11319***

June Park, Euyjin Park, Sungho Kim[…]Hyun-Yong Yu

ACS Applied Materials & Interfaces (2019)

Comments

By submitting a comment you agree to abide by our Terms and Community Guidelines. If you find something abusive or that does not comply with our terms or guidelines please flag it as inappropriate.

Nature

ISSN 1476-4687 (online)

© 2019 Springer Nature Limited